Exchange effects in multisubband plasmons in a quantum well

2001 J. Phys.: Condens. Matter 13 3139

(http://iopscience.iop.org/0953-8984/13/13/322)

INSTITUTE OF PHYSICS PUBLISHING JOURNAL OF PHYSICS: CONDENSED MATTER

J. Phys.: Condens. Matter **13** (2001) 3139–3148 www.iop.org/Journals/cm PII: S0953-8984(01)17377-7

Exchange effects in multisubband plasmons in a quantum well

H Rodríguez-Coppola[1] **and F García-Moliner**

Cátedra de Ciencia Contemporánea, Universitat 'Jaume I', Campus Carretera de Borriol, 12080 Castellón de la Plana, Spain

Received 20 September 2000, in final form 16 February 2001

Abstract

Exchange effects in the intra and intersubband plasmons of a quasi-two-dimensional (Q2D) electron gas confined in a quantum well are studied by means of an extension of the 3D Hubbard dielectric function to the Q2D case. This dielectric function takes full account of the multisubband structure of the spectrum of electronic states. The theory is first tested for semiconductors with a model calculation which yields the expected pattern of behaviour for low electronic densities and then used to study a metallic quantum well. The calculations included a total of ten subbands, seven of them occupied. The main effect of exchange is a tendency to stabilize the plasmon lifetimes against Landau damping. The long wave dispersion relations of the lowest 16 normal modes included in the calculation are also substantially modified.

1. Introduction

The dielectric response of a confined quasi-two-dimensional (Q2D) electron gas has been studied with different models and approximations in inversion layers in MOS structures [1–3] as well as in quantum well (QW) heterostructures [4–14]. The problem has been sometimes studied in the RPA, but some significant advances have been made in the study of many-body interactions beyond the RPA [1, 2, 9–12, 15]. See also [15] for more references on this topic.

Various schemes have been used for this purpose. Thus, in [9] a Bethe–Salpeter approach is employed to study a semiconductor modulation doped QW by including in the analysis two subbands, one occupied and one empty, and some objections are raised against the local density approximation (LDA) favoured by other authors. However, a variant of this approach, denoted the time dependent local density approximation (TDLDA) is used in [11], also with one occupied and one empty subbands in the same type of system, to study the crossover between the plasmon branch and the single-particle excitation continuum. Experiments on a system for which the two-band spectrum is a reasonable approximation [12] appear to be satisfactorily explained on the basis of the TDLDA analysis. An approach somewhat similar in spirit has been used to study parabolic quantum wells with up to four subbands, one occupied and the

[1] Permanent address: Departamento de Física Teórica, Facultad de Física, Universidad de La Habana, Vedado 10400, La Habana, Cuba.

0953-8984/01/133139+10$30.00

rest empty [4]. On the other hand, explicit calculations in the RPA [13, 14] demonstrated the importance of the empty subbands and indicated that the inclusion of several of these above the Fermi level may have significant effects.

Furthermore, in actual systems one may in fact encounter more than one occupied subband. Thus the total number of subbands involved in the analysis may become substantial, depending on the system. In particular, in the metallic QW previously studied in the RPA [10, 14] and presently to be discussed here in a more advanced approximation, there are seven occupied subbands, to which one must add the number of empty subbands one decides to include in the calculation.

Now, in a previous publication [15] the standard Hubbard approximation designed to include exchange interactions in 3D [16] was extended to the case of arbitrary multisubband Q2D systems by developing Hubbard's exchange diagrammatic scheme for this situation, thus deriving the intra- and inter-subband local field correction factors and hence the multisubband Hubbard polarizability and dielectric functions. This is different in spirit from the TDLDA kind of approach, in which the dynamical response theory is essentially RPA while exchange and correlation effects are included in the selfconsistent calculation of electronic eigenstates. In this frame it is observed for the case studied in [11] that some selfconsistency is needed to satisfy some formal requirements of the theory, e.g. current conservation. In the Hubbard approach in 3D [16] exchange interactions are included in the dynamical response theory, leading to a different formula for the polarizability which includes the exchange local field correction. The energies appearing in the final result are formally the renormalized one-electron energies which contain the exchange selfenergy contribution but it is argued [16] that for practical calculations these can be omitted with no significant consequences. The Hubbard dielectric function for Q2D multisubband systems [15] is totally akin to the standard one employed to study (one-band) 3D systems.

The purpose of this paper is to study the effects of exchange in multisubband systems. To this effect some results are presented for plasmon modes in quantum wells obtained from the nonlocal, 2D wavevector and frequency dependent dielectric function $\epsilon(\boldsymbol{q}, \omega; z, z')$ derived in [15]. Section 2 discusses the limit $q \to 0$ for a model semiconductor case with a total of four bands (one occupied), while the main thrust of the paper is contained in section 3, which studies a metallic QW previously studied in the RPA [10, 14], by including in this case a total of ten bands (seven occupied). Final comments are made in section 4.

2. Semiconductor quantum well: study of a model case

We start with a brief reminder of the previous results on which this work is based. Quite generally [13] we start from indices n or m labelling subbands of one-electron states and introduce condensed indices $\mu = (nm)$, denoted with Greek letters, to label pairs of subbands. In terms of the long range ($\mathcal{L}_\mu(\boldsymbol{q}, z)$) and short range ($\mathcal{S}_\nu(z)$) functions introduced in [13] we define in the μ, ν scheme a matrix $\boldsymbol{\beta}(\boldsymbol{q})$ of elements

$$\beta_{\mu,\nu}(q) \equiv \langle \mathcal{L}_\mu(q, z) | \mathcal{S}_\nu(z) \rangle \equiv \int \mathrm{d}z \left[\frac{2\pi}{q} \int \mathrm{d}z' \, \mathrm{e}^{-q|z-z'|} \mathcal{S}_\mu(z') \right] \mathcal{S}_\nu(z) \tag{1}$$

where, for $\mu = (nm)$ and $\nu = (n'm')$, the short range function is

$$\mathcal{S}_\nu(z) = \mathcal{S}_{n'm'}(z) = \varphi_{n'}(z)\varphi_{m'}(z) \tag{2}$$

the function $\varphi_{n'}(z)$ being the z-dependent part of the electronic wavefunction in subband n', and the long range function is the term in square brackets. In order to indicate the label scheme in which different quantities may be cast we shall use the comma only to separate Greek indices or their numerical values.

Then, if $\boldsymbol{\mathcal{L}}/\boldsymbol{\mathcal{S}}$ is the row/column vector of components $\mathcal{L}_\mu/\mathcal{S}_\nu$, the dielectric function is

$$\epsilon(\boldsymbol{q}, \omega; z, z') = \boldsymbol{\mathcal{L}}(\boldsymbol{q}; z) \cdot \boldsymbol{\epsilon}(\boldsymbol{q}, \omega) \cdot \boldsymbol{\mathcal{S}}(z'). \tag{3}$$

Thus, in the dual basis of the functions $\mathcal{L}_\mu$ and $\mathcal{S}_\nu$ the nonlocal function ε is represented by a matrix which, in this scheme, is

$$\boldsymbol{\epsilon}(\boldsymbol{q}, \omega) = \boldsymbol{\beta}^{-1}(\boldsymbol{q}) - \boldsymbol{P}(\boldsymbol{q}, \omega) \tag{4}$$

where $\boldsymbol{\beta}$, defined by (1), represents Coulomb interactions and depends on the spectrum of electronic states, while $\boldsymbol{P}$ is the polarization—a diagonal matrix in the (μ, ν) scheme—which depends on the approximation. In the RPA [13]

$$P^{\mathrm{R}}_\mu(\omega, \boldsymbol{q}) = X_{nm}(\omega, \boldsymbol{q}) + X_{mn}(\omega, \boldsymbol{q}) \tag{5}$$

where

$$X_{nm}(\omega, \boldsymbol{q}) = \frac{2e^2}{\epsilon_o A} \sum_{\boldsymbol{\kappa}} \frac{f_{\boldsymbol{\kappa}+q,m} - f_{\boldsymbol{\kappa},n}}{\mathcal{E}_{\boldsymbol{\kappa}+q,m} - \mathcal{E}_{\boldsymbol{\kappa},n} + \hbar\omega^+} \tag{6}$$

and the symbols have the well known standard meaning with details adapted to the Q2D case: thus $\boldsymbol{\kappa}$ and $\boldsymbol{q}$ are 2D, A is a normalization area and $\boldsymbol{\kappa}$ and n label the state of 2D momentum $\boldsymbol{\kappa}$ in subband n.

The polarizability elements in the Q2D Hubbard approximation [15] are

$$\boldsymbol{P}^{\mathrm{H}}(\boldsymbol{q}, \omega) = \| P^{\mathrm{H}}_\mu(\boldsymbol{q}, \omega)\delta_{\mu,\nu} \| = \left\| \left(\frac{P^{\mathrm{R}}_\mu(\boldsymbol{q}, \omega)}{1 + H_\mu(\boldsymbol{q}) P^{\mathrm{R}}_\mu(\boldsymbol{q}, \omega)} \right) \delta_{\mu,\nu} \right\| \tag{7}$$

where

$$H_\mu(q) = \beta_{\mu,\mu}(q) G\mu(q) \qquad G_\mu(q) = \frac{\beta^{\mathrm{x}}_{\mu,\mu}(q')}{2\beta_{\mu,\mu}(q)}. \tag{8}$$

The cross in the β term in the numerator denotes the result of the multisubband Hubbard approximation, for which, with $\mu = (nm)$,

$$\beta^{\mathrm{x}}_{\mu,\mu}(q') \equiv \langle \mathcal{L}_{mm}(q', z) | \mathcal{S}_{nn}(z) \rangle \qquad q' = \sqrt{q^2 + \kappa_F^2/2} \tag{9}$$

where κ_F is the Fermi radius of the first occupied subband. Note the differences with respect to (1): (i) β^{x} is evaluated for q', not for q, and (ii) subband indices are exchanged so $\mathcal{L}_{nm}$ and $\mathcal{S}_{nm}$ are changed into $\mathcal{L}_{mm}$ and $\mathcal{S}_{nn}$. Written in this way $G_\mu(q)$ is the local field correction accounting for exchange interactions between the two subbands with labels n and m—which may be equal or different—condensed in μ and then all the matrix algebra is done with matrices of rank 2 in the μ, ν scheme.

One way to obtain the plasmon dispersion relation is to calculate the roots of the secular determinant, i.e. $\det|\epsilon_{\mu,\nu}|$. Another way [14] is to study the peaks of the loss function, essentially $\mathrm{Im}\{\epsilon^{-1}\}$, which involves inverting the matrix (4). In practice it proves convenient to combine both methods for cross checking dubious cases and resolving ambiguities. The latter also provides a convenient way to study the lifetime of the normal modes, as will be seen in section 3.

While the main purpose is to study metallic QWs, for which the simple square infinite well is even a reasonable model, we shall first investigate with this model some general features of semiconductor systems. While this would be inappropriate to attempt a realistic calculation for a specific case, it suffices for the present purpose as it serves to make some connection with other studies of semiconductor systems [11] and to set out the pattern for the more complicated metal case involving ten subbands altogether.

We now consider an infinite square well with one occupied subband and include three empty subbands above. Due to the symmetry of the system, the space of solutions is factorized as the direct product of symmetric (S) and antisymmetric (A) subspaces and then, in the μ, ν scheme, the total matrices are block-diagonalized accordingly. Following the pattern set out in [13], the assignment of (nm) pairs to the μ indices in each subspace is as shown in table 1.

Table 1. Assignments μ:(nm) for the symmetric (S) and antisymmetric (A) subspaces in a four-band approximation with one occupied subband.

μ^S	n	m	μ^A	n	m
1	1	1	1	2	1
2	3	1	2	4	1

In each subspace the $\epsilon_{\mu,\nu}$ matrix is 2×2 and the secular equation is

$$\det \begin{vmatrix} (\beta^{-1})_{1,1} - P_1 & (\beta^{-1})_{1,2} \\ (\beta^{-1})_{2,1} & (\beta^{-1})_{2,2} - P_2 \end{vmatrix} = 0 \tag{10}$$

with the μ, ν indices referring to subband pairs as shown in table 1 for each case. Thus a study involving a total of four subbands can be carried out analytically if desired.

We concentrate on the intersubband modes, which for typical semiconductor systems exhibit the more meaningful consequences of many-body interactions [11], and study the limit $q \to 0$. The secular determinant (10) for the symmetric subspace has two roots. One is the intrasubband {11} mode. The other one is the intersubband {31} mode, for which the plasmon energy is, at $q = 0$:

$$E_p = \hbar\omega = \gamma_{31}\sqrt{\Gamma_2 + \frac{t|\sigma_{2,2}|}{\Gamma_2}} \tag{11}$$

where $\gamma_{31} = E_3 - E_1$ is the single-particle excitation energy from subband 1 to subband 3 with the same 2D wavevector and the definition

$$t = \frac{2m^*e^2}{\pi\epsilon_o\hbar^2}$$

is used. The term $\sigma_{2,2}$ results from the low q expansion and is generally defined by

$$\sigma_{\mu,\nu} = 2\pi \int \mathrm{d}z \mathcal{S}_\nu(z) \int \mathrm{d}z' |z - z'| \mathcal{S}_\mu(z'). \tag{12}$$

In this case $\mu = \nu = 2$, which from table 1 couples subbands 1 and 3 and

$$\Gamma_2 = 1 - t\beta^{\mathrm{x}}_{2,2}(\kappa_F/\sqrt{2}) \tag{13}$$

where $\beta^{\mathrm{x}}_{2,2}$ is the exchange term defined in (9) for arbitrary μ, here specified for $\mu = 2$ of the S subspace, and evaluated for $q = 0$, so $q' = \kappa_F/\sqrt{2}$.

The antisymmetric modes are likewise studied. In this case the two modes are intersubband, coupling subbands 2 and 1 for $\mu = 1$ and 4 and 2 for $\mu = 2$. The secular determinant in the limit $q \to 0$ is

$$\begin{vmatrix} -\sigma_{2,2} + ((t\Delta\gamma_{21}^2)/\Gamma_1)/(\gamma_{21}^2\Gamma_1 - E_p^2) & \sigma_{1,2} \\ \sigma_{2,1} & -\sigma_{1,1} + ((t\Delta\gamma_{41}^2)/\Gamma_2)/(\gamma_{41}^2\Gamma_2 - E_p^2) \end{vmatrix} = 0 \tag{14}$$

where E_p is the plasmon energy for $q \to 0$ and $\Delta = \sigma_{1,1}\sigma_{2,2} - \sigma_{1,2}\sigma_{2,1}$. When exchange interactions are switched off, then all $\beta^{\mathrm{x}}_{\mu,\mu}$ vanish, all Γ_μ equal unity and we recover the RPA in all cases.

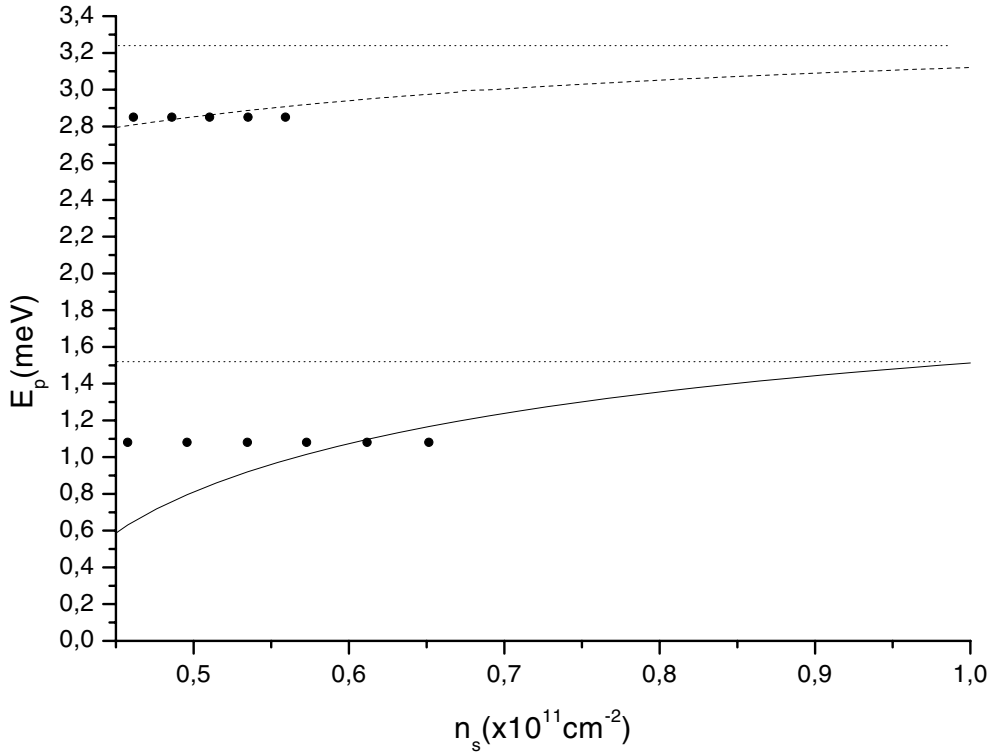

Figure 1. The plasmon energy $E_p(q \to 0)$ for two intersubband modes of the infinite square well with one occupied and three empty subbands discussed in the text, as a function of the electron areal density n_s in units of 10^{11} cm^{-2}. Results obtained from the dielectric function in two approximations. Full line: Q2D Hubbard [15] for plasmon {21} (antisymmetric mode). Dashed line: Q2D Hubbard for plasmon {31} (first symmetric mode). Dotted line: Q2D RPA [13] for the two modes. The dots show the single particle excitation energy $\gamma_{n1} = E_n - E_1$ for the two modes.

Figure 1 shows the plasmon energy $E_p(q \to 0)$ for the two lowest intersubband—{21} and {31}—modes of a 400 Å wide GaAs well as a function of electron areal density n_s, which we explore in the range of values slightly below 10^{11} cm^{-2}. In qualitative agreement with the findings of [11] in about the same range, the picture emerging from these results is as follows. In the RPA, Coulomb depolarizing field effects raise the value of $E_p(0)$ above the single-particle excitation energy γ_{n1}. Then, as exchange interactions are switched on, excitonic effects lower E_p below the RPA value. Starting from the right-hand side of the figure, E_p is at first above γ_{n1} and then, as n_s is lowered, E_p decreases, crosses the value γ_{n1} and from then on lies below the single-particle excitation energy.

Now, the qualitative and even semi-quantitative agreement with the pattern first observed in [11] is very interesting. The two calculations are quite different in every respect, from the details of the QW under study to the approach, formalism and approximations involved. For instance, in [11] an effort is made to build up a realistic model, the monoelectronic states are calculated within the TDLDA including a local functional of exchange and correlation in the calculation; with them the dielectric response is obtained within the RPA. On the other hand, in the present model calculation the monoelectronic states are calculated only in the Hartree approximation (without any renormalization) and the dielectric response is obtained considering the contribution of exchange. Yet the pattern is the same and even the range of

values of n_s where the significant changes appear is roughly in the same order of magnitude, which suggests that this is an inherent feature, in a first approximation fairly insensitive to details and such that exchange interactions essentially suffice to account for it. Having seen how the Q2D multisubband Hubbard approximation works in practice, we now move on to the main subject of our calculations, which is the study of metallic QWs where the number of subbands involved is much larger.

3. Metallic quantum well

We consider the QW studied in [10, 14]. This is a 20 Å thick metallic well embedded in a dielectric matrix. The first quantized energy level is $E_1 = 94$ meV, the areal electron density is $n_s = 2, 16.10^{15}$ cm^{-2} and there are seven occupied subbands. The effect of including higher, empty subbands was explicitly studied for plasmon modes in [14], where the difference between the results obtained with and without such higher terms was found to be very substantial even for modes associated with the lower subbands. This in turn, is in line with the conclusions reached in [13] in the study of the dynamical screening of an external potential. This will not be discussed here any further in explicit form. We shall simply present some results obtained in the calculation involving a total of ten subbands, seven occupied and three empty. We employed an infinite square well, which, for the metallic case, is even a reasonable model. We use the μ, ν scheme as in section 4 and find, for the symmetric and antisymmetric subspaces the $\mu : (nm)$ assignments as shown in table 2.

Table 2. Assignments μ:(nm) for the symmetric (S) and antisymmetric (A) subspaces for a well with seven occupied and three empty subbands.

μ^S	n	m	μ^S	n	m	μ^A	n	m	μ^A	n	m
1	1	1	9	4	2	1	2	1	9	5	2
2	2	2	10	5	3	2	3	2	10	6	3
3	3	3	11	6	4	3	4	3	11	7	4
4	4	4	12	7	5	4	5	4	12	8	5
5	5	5	13	8	6	5	6	5	13	9	6
6	6	6	14	9	7	6	7	6	14	10	7
7	7	7		...		7	8	7		...	
8	3	1				8	4	1			

Figure 2 shows the plasmon dispersion relations in the low q range for the first 11 symmetric modes. Of these, the first seven are intrasubband and correspond to $\mu^s = 1, \cdots, 7$, in the same order, in table 2. The next four are intersubband and correspond to $\mu^s = 8, \cdots, 11$. The situation is now considerably more complex. The dynamical equations leading to the Q2D Hubbard approximation for ϵ contain always two types of term having the nature of electrostatic and excitonic interactions. In a simple case, with only two bands, the effects of these can be neatly separated and the final result explained as an algebraic sum of two effects with opposite signs [11], as discussed in section 2. However, with a large number of subbands involved, while the various terms retain their original sign and meaning, their products combine in a complicated way in a large determinant and a neat separation of the opposite effects becomes impossible. The only way is to do the numerical calculation and examine the results.

These are given in the form of dispersion relations in figure 2 for the first 11 symmetric modes, as explained, and in figure 3 for the first five antisymmetric ones, obviously the latter are all intersubband and correspond to $\mu^A = 1, \cdots, 5$ in table 2. For this system the effects of exchange are everywhere significant and actually rather more complicated, as expected. The

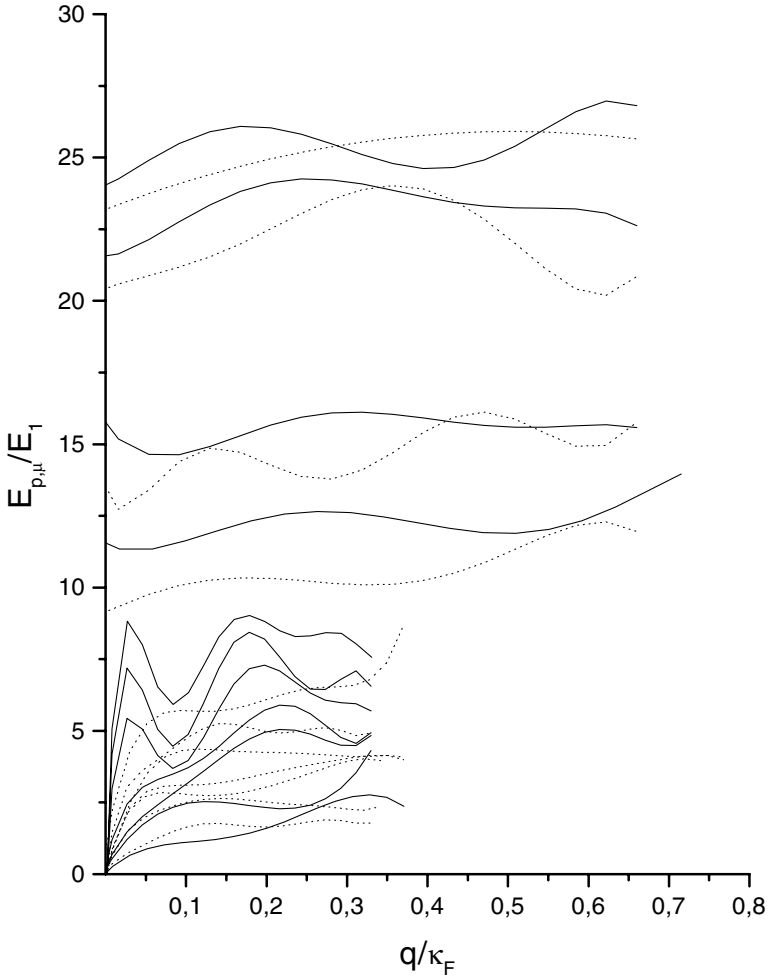

Figure 2. Dispersion relations for the first 11 symmetric normal modes, corresponding to $\mu^s = 1, \cdots, 11$ in table 2, for the metallic quantum well discussed in the text. The first seven—$\mu^s = 1, \cdots, 7$—are intrasubband and the next four modes—$\mu^s = 8, \cdots, 11$—are intersubband. Results obtained from the Q2D multisubband dielectric function in two approximations. Dashed lines: RPA. Full lines: Hubbard approximation.

Hubbard result—full lines—may actually be below or above the RPA value, depending on q. We also note that many intersubband branches have a negative dispersion range, a feature also found in [11] and in the simple model calculation described—though not explicitly displayed—in section 3.

Now, seen in terms of $\mathrm{Im}\{\epsilon^{-1}\}$ the dispersion relations only show the evolution of the peak positions as a function of q for the different branches. But one of the purposes of the present analysis is to investigate to what extent different electron–electron interactions may affect differently the decay of the plasmon modes in single particle excitations. This can be ascertained from the evaluation of the spectral function $-\mathrm{Im}\{\epsilon^{-1}\}$, either as a function of q for fixed ω or *vice versa*. The second alternative was chosen for the results shown in figure 4, spanning the low frequency range $0 < \hbar\omega < 15\ E_1$ for $q = 0.16\ \kappa_F$. A comment is in order here. When only one band is involved, then the only plasmon damping at $T = 0$ K is due to

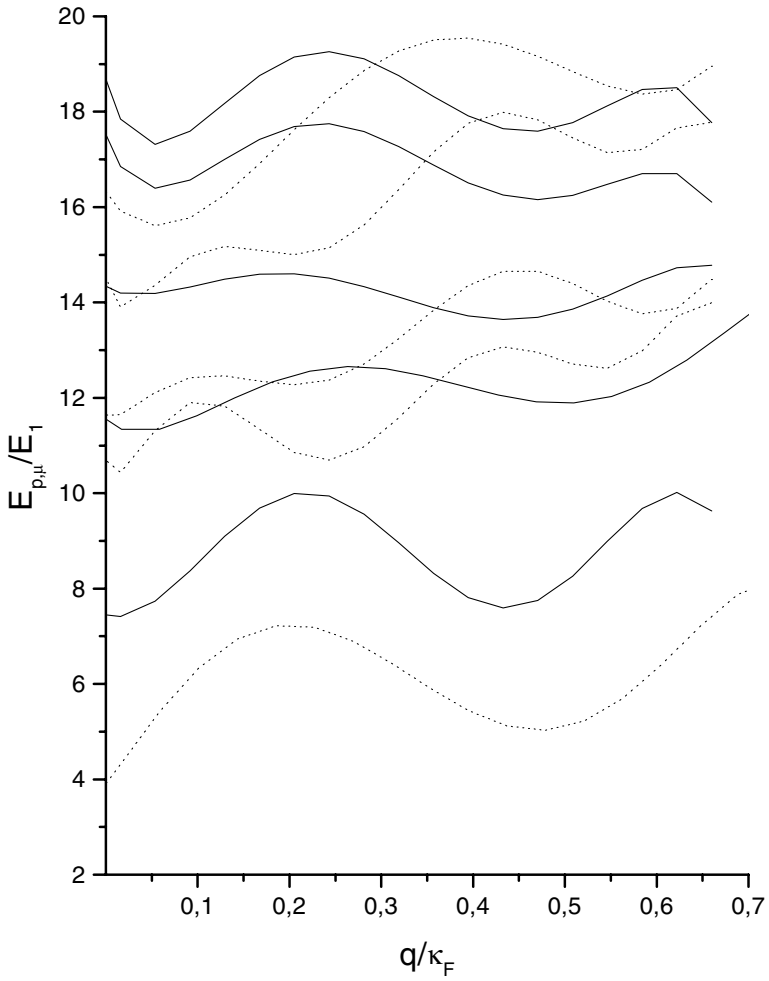

Figure 3. Dispersion relations for the first five antisymmetric intersubbands normal modes—$\mu^A = 1, \cdots, 5$ in table 2—for the same system as in figure 2.

the incoherent single-particle excitation (Landau) damping. The mode is then stable before the dispersion branch enters the Landau region. This picture does not provide a sufficiently complete description of the situation when several subbands are involved. The point is that several intersubband pairs are simultaneously involved in the various excitations and a given collective mode $\{nm\}$ dispersion branch may enter other $\{n'm'\}$ Landau regions before it enters the one corresponding to n and m and indeed may often be simultaneously inside different Landau regions. This mutual coupling of several intersubband excitations which participate simultaneously in the process, results in more complicated and less conventional damping patterns, depending on the values of ω and q. In the case of figure 4 all plasmon dispersion branches are practically always inside Landau damping regions, but the two approximations behave very differently, the decay of the collective modes being considerably stronger in the RPA. When exchange interactions are included the coupling between collective and single-particle modes is weaker. The signal to noise ratio is much weaker in the RPA than in the present calculation. Even for this not so low value of q we still find recognizable peak features

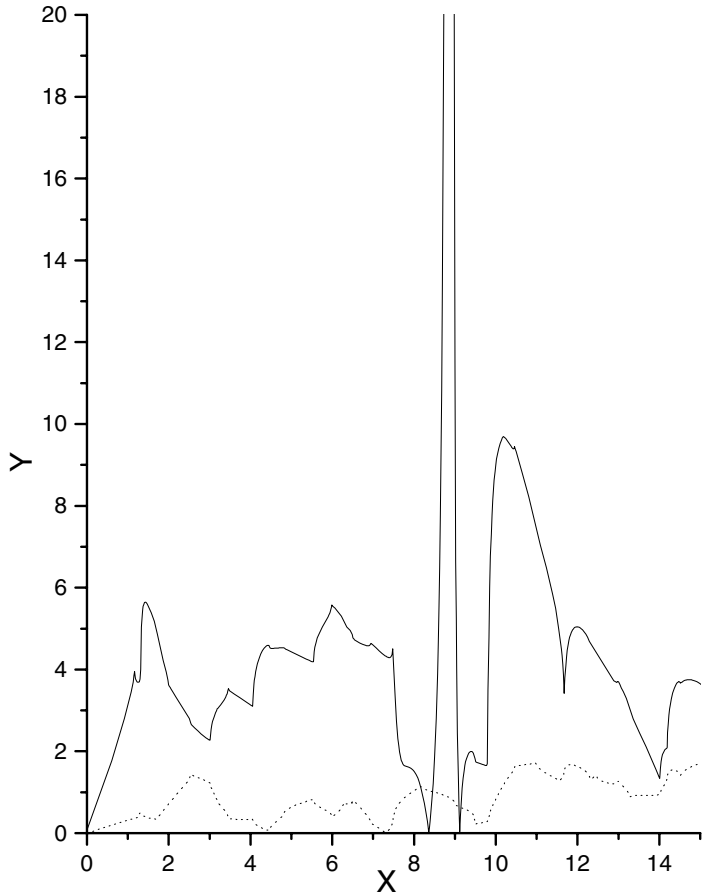

Figure 4. The spectral function $Y = -\mathrm{Im}\{\epsilon^{-1}\}$ as a function of dimensionless frequency variable $X = \hbar\omega/E_1$, spanning the range $0 < X < 15$ for fixed $q = 0.16\ \kappa_F$. The system is the same as in figures 2 and 3. The spectral strength includes the entire spectral range—symmetric and antisymmetric modes—and the meaning of full and dashed lines is also as in figures 2 and 3.

and a distinctly sharp peak. The details may differ for different specific cases, but these results suggest that the exchange interactions tend to stabilize the collective normal modes as the exclusion principle operates more explicitly and imposes more stringent restrictions on the disruptive effects of incoherent single particle excitations.

Needless to say, on doing numerical calculations one adds in practice a very small imaginary part to the real energy variable, but this is quantitatively irrelevant.

4. Conclusions

Exchange interactions in the dielectric response of a confined electron gas in systems like a QW can be studied by means of the formal extension of the Hubbard approximation to the Q2D multiband case. This has been used here to study plasmon normal modes. While a realistic calculation for semiconductor QWs would require taking account of important details, like e.g. the shape of the potential well due to modulation doping with all its consequences, a simple model calculation for an infinite rectangular well suffices to bear out the main features.

For a simple situation, with one occupied and one empty subband it is possible to see the interplay of Coulomb depolarizing field effects, which raise the normal mode frequency, and the opposite effect of exchange interactions, in agreement with other calculations based on different approaches designed to be more realistic and including exchange and correlation. The agreement is not only qualitative but also semiquantitative as regards the general trend as a function of decreasing n_s in the low density range. This is somewhat remarkable in view of the simplicity of the idealized exercise carried out here and suggests (a) that this trend is an inherent basic feature of low density systems which appears to be fairly insensitive to the details of the calculation and the approximation involved and (b) that exchange interactions essentially suffice to account for it.

The main purpose of the work here described is to study the effects of exchange on both the dispersion and the damping of plasmon modes in systems involving a large number of subbands. This has been done here by means of the Q2D Hubbard dielectric function described in the text. For a metallic quantum well with seven occupied subbands we have included three empty ones; with a total of ten subbands involved in the analysis the picture is a rather complicated one and the consequences of direct electrostatic and excitonic interactions can no longer be interpreted as a linear combination of two opposite effects. The result, seen in figures 2 and 3, is that the plasmon frequency in the Q2D Hubbard approximation may end up above or below the RPA result, depending on q.

The most explicit differences between the two approximations lie in the lifetime of the collective normal modes, which exchange interactions tend to stabilize on account of the more explicit role of the exclusion principle, which tends to hinder the disruptive effects of the incoherent single-particle excitations.

Acknowledgments

This work was largely carried out while one of the authors (HR-C) was enjoying a Sabbatical grant SAB1995-0733 of the Spanish Ministry of Education and Science and completed with a grant INV00-15-59 of the 'Generalitat Valenciana'.

References

[1] Vinter B 1976 *Phys. Rev.* B **13** 4447
Vinter B 1977 *Phys. Rev.* B **15** 3947
[2] Ando T, Fowler A and Stern F 1982 *Rev. Mod. Phys.* **54** 437
[3] Tsellis A, Gonzales de la Cruz G and Quinn J J 1983 *Solid State Commun.* **46** 779
[4] Wendler L and Pechstedt R 1986 *Phys. Status Solidi* b **138** 197
[5] Eliasson G, Hawrylak P and Quinn J J 1987 *Phys. Rev.* B **36** 7631
[6] Ehlers D H 1988 *Phys. Rev.* B **38** 9706
[7] Streight S R and Mills D L 1989 *Phys. Rev.* B **40** 10 488
[8] Fassol G, King-Smith R D, Richards D, Ekenberg U, Mestresand N and Ploog K 1989 *Phys. Rev.* B **39** 12 695
[9] Chuang S L, Luo M S C, Schmitt-Rink S and Pinczuk A 1992 *Phys. Rev.* B **46** 1897
[10] Backes W H, Peters F M, Brosens F and Devreese J T 1992 *Phys. Rev.* B **45** 8437
[11] Marmorkos I K and Das Sarma S 1993 *Phys. Rev.* B **48** 1544
Das Sarma S and Marmorkos I K 1993 *Phys. Rev.* B **47** 16 343
[12] Ernst S, Goñi A R, Syassen K and Eberl K 1994 *Phys. Rev. Lett.* **72** 4029
[13] Fernández-Velicia J, García-Moliner F and Velasco V R 1996 *Phys. Rev.* B **53** 2034
[14] León-Monzón K, Rodríguez-Coppola H, Velasco V R and García-Moliner F 1996 *J. Phys.: Condens. Matter* **8** 665
[15] Rodríguez-Coppola H, García-Moliner F and Velasco V R 2000 *Phys. Scr.* **61** 200
[16] Mahan D G 1990 *Many-Particle Physics* (New York: Plenum)
[17] Fernández-Velicia J, García-Moliner F and Velasco V R 1995 *J. Phys. A: Math. Gen.* **28** 391